Available online at www.sciencedirect.com
ScienceDirect
Journal of Photochemistry and Photobiology B: Biology 85 (2006) 216–222
Journal of Photochemistry and Photobiology B:Biology
www.elsevier.com/locate/jphotobiol

Effect of nanoparticle size on the extravasation and the photothrombic activity of *meso*(*p*-tetracarboxyphenyl)porphyrin

Bernadette Pegaz, Elodie Debefve, Jean-Pierre Ballini, Yvette Niamien Konan-Kouakou, Hubert van den Bergh *

Ecole Polytechnique Federale de Lausanne (EPFL), Faculté des Sciences de base, Laboratory of Photomedicine, Station 6, CH-1015 Lausanne, Switzerland

Received 9 January 2006; received in revised form 10 July 2006; accepted 22 July 2006
Available online 18 September 2006

Abstract

Particle size should be optimized to achieve targeted and extended drug delivery to the affected tissues. We describe here the effects of the mean particle size on the pharmacokinetics and photothrombic activity of *meso-tetra*(carboxyphenyl)porphyrin (TCPP), which is encapsulated into biodegradable nanoparticles based on poly(D,L-lactic acid). Four batches of nanoparticles with different mean sizes ranging from 121 to 343 nm, were prepared using the emulsification–diffusion technique. The extravasations of each TCPP-loaded nanoparticle formulation from blood vessels were measured, as well as the extent of photochemically induced vascular occlusion. These preclinical tests were carried out in the chorioallantoic membrane (CAM) of the chicken's embryo. Fluorescence microscopy showed that both the effective leakage of TCPP from the CAM blood vessels and its photothrombic efficiency were dependent on the size of the nanoparticle drug carrier. Indeed, the TCPP fluorescence contrast between the blood vessels and the surrounding tissue increased at the applied conditions, when the particle size decreased. This suggests that large nanoparticles are more rapidly eliminated from the bloodstream. In addition, after injection of a drug dose of 1 mg/kg body weight and a drug-light application interval of 1 min, irradiation with a fluence of 10 J/cm^2 showed that the extent of vascular damage gradually decreased when the particle size increased. The highest photothrombic efficiency was observed when using the TCPP-loaded nanoparticles batch with a mean diameter of 121 nm. Thus, in this range of applied conditions, for the treatment of for instance a disease like choroidal neovascularization (CNV) associated with age-related macular degeneration (AMD), these experiments suggest that the smallest nanoparticles may be considered as the optimal formulation since they exhibited the greatest extent of vascular thrombosis as well as the lowest extravasation.

Keywords: Photodynamic therapy; Photosensitizer; *meso-tetra*(carboxyphenyl)porphyrin; Chicken embryo; Nanoparticles; Particle size

1. Introduction

Photosensitizers (PS) are light activated drugs used clinically on a large scale among others in photodynamic therapy (PDT) applied to treat choroidal neovascularization (CNV) associated with age-related macular degeneration (AMD) [1–3], and to treat cancer.

A number of reports comparing the PDT outcome of intravenously (i.v.) injected nanoparticles (NPs) loaded with photosensitizer versus free injected photosensitizer under otherwise identical conditions provide strong evidence that a PS in NP formulation might be preferred for the treatment of disease [4–7]. Many different approaches using various physical and biochemical principles have been proposed and examined to develop a way to achieve a therapeutically acceptable degree of disease targeting. Recently, the rationale of the NP delivery approach has been established in various systems among which EMT-6 mammary tumor cells and rhabdomyosarcoma-bearing DBA/2 mice [8]. The goal of the present work was to develop a suitable nanoparticle polymeric drug delivery system loaded with photosensitizer.

* Corresponding author. Tel.: + 41 21 693 36 23; fax: + 41 21 693 36 26.
E-mail address: hubert.vandenbergh@epfl.ch (H. van den Bergh).

1011-1344/$ - see front matter © 2006 Elsevier B.V. All rights reserved.
doi:10.1016/j.jphotobiol.2006.07.008

The nanoparticles are to be i.v. injected. They should not leak out of the vasculature to a significant extent on the time scale of the treatment, and if possible this procedure should enhance the photodynamic activity of the photosensitizer. Biodegradable and biocompatible NPs based on poly(D,L-lactide) were chosen as delivery system. One can speculate that the efficiency of target vascular damage due to PDT with nanoparticle delivered photosensitizer is determined by the properties of the nanocarriers including their mean size, as the latter may well play an important role in the cellular and tissular uptake. Consequently, NPs with four different mean sizes were prepared using the emulsification–diffusion technique. The resulting NP formulations were characterized regarding their size distribution, as well as their drug loading and the entrapment efficiency. The size dependence of extravasation and photothrombic activity of NPs was then investigated in vivo using the chick's chorioallantoic membrane (CAM) as a model [9–11]. This model was chosen because cell culture studies do not give any insight into vascular photothrombosis. In our assays with the CAM model as an in vivo assay for PDT, the photosensitizer was i.v. administrated [12,13]. We choose one of the PS studied in a former work [6], with the idea to maintain unchanged all PDT parameters, while varying only the particle size.

It may be noted that the CAM has received considerable attention in research on angiogenesis. The CAM is the major respiratory organ of the chick embryo. The well-vascularized surface is formed by the fusion of two mesodermal layers, and has several advantages as a model to assess the vascular damage induced by PDT.

The injection of a fluorescent dye following PDT is used to assess the vascular occlusion. One may note that this procedure is close to the clinical situation, in which one wishes to close CNV associated with AMD, where PDT efficacy is evaluated by fluorescein and/or indocyanine green fluorescence angiography.

2. Materials and methods

2.1. Materials

Poly(D,L-lactide) (Resomer® R202H) with a molecular weight of approximately 12,000 Da was obtained from Boehringer Ingelheim (Ingelheim, Germany). The photosensitizer, *meso-tetra*-(*p*-carboxyphenyl)porphyrin (TCPP) was obtained from Porphyrin Products (Frontier Scientific, Logan, USA). Poly(vinyl alcohol) (PVAL) 87.7% hydrolyzed with a molecular weight of 26,000 Da (Mowiol®4-88) (Omya AG, Oftringen, Switzerland) and benzyl alcohol (Fluka Biochemika, Buchs, Switzerland) were used as organic solvents for the NP preparation. Phosphate buffer saline (PBS) and Dimethylsulfoxide (DMSO) were provided by Life-Technologies (Basel, Switzerland) and Sigma–Aldrich (Steinheim, Germany), respectively. D(+)-trehalose dihydrate was purchased from Sigma Chemical Co. (St. Louis, MO, USA). Sulforhodamine 101 was purchased from Fluka Biochemika (Buchs, Switzerland). All other chemicals were of analytical grade and were used without further purification.

2.2. Methods

2.2.1. Nanoparticle preparation

The production of small biocompatible organic NPs was investigated using the emulsification–diffusion process [5]. The process parameters were originally chosen following previous work [14–16]. These conditions were then varied in order to investigate their influence on the particle mean size and size distribution. The water used was distilled water that was then deionized (SGwater, Hamburg, Germany, type "UltraClear"). Typically, 5 g of solution containing 190 mg of organic material (R202H) and the PS (10 mg), was added under mechanical stirring to 10 g of an aqueous phase containing PVAL and 60% (w/w) of a salting out agent ($MgCl_2 \cdot 6H_2O$). The emulsification–diffusion method can be considered as a modification of the salting out procedure, but by avoiding the use of salts one avoids subsequent major purification steps. After the formation of an oil-in-water emulsion at room temperature, 60 ml of pure water was added to induce complete diffusion of the solvent into the aqueous phase, which leads to the formation of the NPs. Since the effectiveness of the sterile filtration process is also influenced by the microbial burden of the NP suspension to be filtered, water filtered through a 0.1 μm membrane filter (Millipore, Switzerland) was used for the preparation and the purification of the NPs. The particle size was evaluated as function of (a) the stirring rate (1000–2000 rpm), (b) PVAL percentage (4–15% (w/w)) [17].

2.2.2. Nanoparticle purification

The particle suspensions were purified by cross-flow filtration using a Sartocon® Slice device fitted with an ultrafiltration membrane (Sartorius, Goettingen, Germany). Finally trehalose was added (trehalose:NPs mass ratio of 2:1) as this nonreducing disaccharide exhibits a satisfactory lyoprotective effect for pharmaceutical and biological materials [18–20]. The purified particle suspensions were then frozen and freeze-dried at 0.05 mbar in a Laboratory Dryer "Alpha 1-2 LD" (Martin Christ GmbH, Osterode am Harz, Germany).

2.2.3. Particle size measurement

The mean particle size was assessed by photon correlation spectroscopy using a "Zetasizer® 3000 HS" (Malvern Instruments Ltd., Worcestershire, England).

The amount of the PS loaded in the NPs was determined spectrophotometrically by the absorption at 420 nm. To accomplish this, a known amount of freeze-dried photosensitizer encapsulated NPs was completely dissolved in DMSO and the absorbance due to the PS was then measured in the Soret band at 420 nm. Encapsulation efficiency was then calculated based on the ratio of the amount of PS incorporated into the NPs as compared to the amount of PS used in the initial mixture. The latter was 5% w/w [5].

2.2.4. Drug loading

The drug loading was calculated according to the weight ratio [21]:

$$\text{Drug loading}(\%) = \frac{\text{weight of drug in the nanoparticles}}{\text{weight of nanoparticles}} \times 100\ (\%).$$

2.2.5. CAM preparation

Fertilized chicken eggs were disinfected and transferred into a hatching incubator set at 37 °C and 60% humidity which was equipped with an automatic rotator (SARL SAVIMAT, Chauffry, France). On the third day of embryo development (EDD3), a hole of approximately 3 mm diameter was bored into the eggshell at the narrow apex and covered with a cling foil. No albumin was aspirated since the egg incubation was continued in a static position, allowing the formation of a flat vascularised membrane within 10 days. On EDD13, the holes were extended to a diameter of about 3 cm, and the embryos were placed under an epi-fluorescence microscope (Nikon Eclipse E600 FN, Japan) equipped with a Nikon objective CFI achromat (magnification 4X, N.A. = 0.10, W.D. = 30 mm) and with an F-view II 12-bit monochrome Peltier-cooled digital CCD camera driven with analySIS® docu software from Soft Imaging System (Münster, Germany). The resulting image-size is 3.51 × 2.81 mm.

2.2.6. Fluorescence pharmacokinetics

The fluorescence pharmacokinetics was performed on the CAM on EDD13 as previously described[12]. Briefly, a volume of 10 μl containing 1 mg/kg body weight (b.w. of the embryo on EDD13 ≈ 10 g) [22] of the PS was i.v. injected under the microscope. Fluorescence imaging was performed using the excitation light of a Hg-arc lamp between 400 and 440 nm. A 650 nm long-pass emission filter was used to observe the fluorescence from the PS and to reject the excitation light. The fluorescence images of the

Table 1
Evaluation of PDT-induced damage on CAM vessels, from Lange et al. [12]

Damage scale[a]	Criterion
0	No damage
1	Partial closure of capillaries with diameter <10 μm
2	Closure of the capillary system and partial closure of blood vessels of diameter <30 μm, together with size reduction of larger blood vessels
3	Closure of vessels of diameter <30 μm, and partial closure of higher order vessels
4	Total closure of vessels of diameter <70 μm, and partial closure of larger vessels
5	Total occlusion of vessels in the irradiated area

Image below to illustrate which size of vessels are taken into account in this damage evaluation. Image size is 3.51 × 2.81 mm.

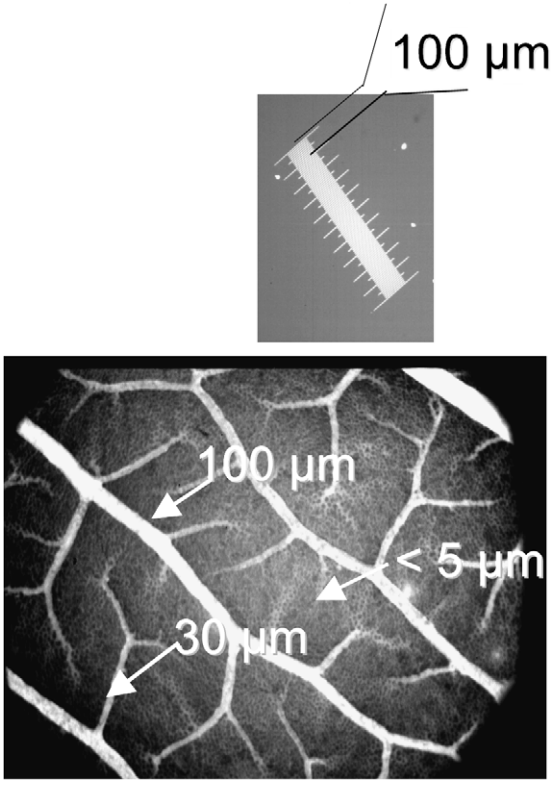

[a] Intermediate values are found when making the average of different scores.

CAM surface were recorded at regular time intervals, for approximately 30 min after injection. The time-dependent evolution of the fluorescence intensity inside the blood vessels (I_{in}) with respect to the fluorescence intensity of the surrounding tissue (I_{out}) was expressed by means of normalized photographic contrast C_{phot}:

$$C_{phot} = \frac{(I_{in} - I_{out})}{(I_{in} + I_{out})} \times (1/C_{phot,max})$$

where $C_{phot,max}$ represents the highest photographic contrast following administration of the PS.

At least five embryos were injected for each experimental condition.

2.2.7. Photodynamic therapy

Also on EDD 13 in parallel to the fluorescence pharmacokinetics measurements mentioned above, PDT was carried out. For this purpose another set of five eggs per set of NP parameters were placed under the microscope. The treatment area, which is the area to be illuminated, was chosen and labeled by placing a small Teflon ring (5 mm in diameter) on the CAM, in order to more easily recover it for the control occurring the following day. Prior to drug injection, an autofluorescence image of the CAM surface was recorded in order to verify the autofluorescence background level. Subsequently, injection of a dye dose of 1 mg/kg b.w. was performed in situ under the microscope, and the circulation of the PS was observed by fluorescence microscopy. Following the initial apparently homogenous distribution of the PS in the blood circulation, which was observed about one minute after the i.v. injection, PDT was performed using a filtered Hg-arc lamp with light in the range 400–440 nm, at a fluence rate of 141 mW/cm^2. Irradiations with a fluence of 10 J/cm^2 were applied to the CAM, on a area of diameter 1.75 mm limited by an excitation diaphragm. The eggs were then covered with a cling foil and returned to the incubator for 24 h. Then PDT induced vascular occlusion was measured by means of fluorescence angiography. The latter was performed by injection of 10 μl of an aqueous solution of sulforhodamine 101 (5 mg/ml). Fluorescence angiographies, pre- and post- PDT, were compared and vessel closure was scored following an arbitrary scale (Table 1) [12]. Furthermore, by comparing the irradiated area to the surrounding non-irradiated areas, we were able to quantitatively assess the effect on the blood vessels of the PS by itself without light exposure (i.e. dark toxicity). At least five eggs were used per measurement condition, and the resulting photothrombic efficiency was given as the average of the closure level.

3. Results and discussion

3.1. Influence of the stirring rate on particle size

The viscosity of the aqueous phase known to be an important factor influencing the particles parameters, can be varied by the concentration and/or the molecular weight of the PVAL used [14,23]. It has been reported that NP with a mean size in the 100 nm range can be obtained using the emulsification–diffusion technique by raising the percentage of PVAL and using a somewhat low stirring rate (2000 rpm, compared to 5000 rpm used by Leroux et al.) [23]. Accordingly, as can be seen in Fig. 1, the mean size of the nanoparticles decreased when the stirring rate was increased in the range from 1000 to 2000 rpm, while increasing the percentage of the stabilizing agent Mowiol from 4 to 15%. Four batches of TCPP-loaded NPs were prepared with an initial drug loading of 5% (w/w) using the emulsification–diffusion technique. As shown in Table 2, nanoparticles as small as 121 nm in diameter, with a narrow size distribution could be obtained reproducibly. Somewhat surprisingly, we found that both the drug loading (PS vs NP w/w) and the efficiency of the entrapment (part of the initial PS, loaded in the NP at the end of the process) were independent of the mean particle size. Indeed, irrespective of the mean particle size, a drug

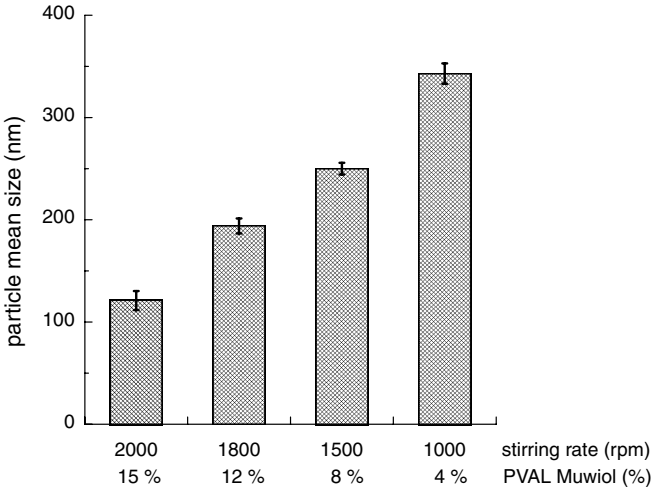

Fig. 1. Influence of the stirring rate and of the percentage of PVAL (Mowiol® 4–88) in the solutions, on the mean size of TCPP-loaded R202H nanoparticles. Error bars on the NP mean size represent the 67% confidence level from 5 measurements.

Table 2
Characterization of TCPP-loaded nanoparticles freeze-dried in presence of trehalose (mean ± SD, $n = 3$)

Mean particle size (nm)	Polydispersity index (PI)	Drug loading w/w (%)[a]	Entrapment efficiency (%)[b]
121 ± 10	0.42	0.9 ± 0.1	18.8 ± 1.2
194 ± 12	0.21	1.07 ± 0.08	20.9 ± 0.5
250 ± 5	0.30	1.0 ± 0.1	20.3 ± 2.0
343 ± 10	0.23	1.2 ± 0.1	23.7 ± 1.6

[a] In the initial mixture, the amount of drug versus nanoparticles was 5% w/w.
[b] Part of the initial drug, loaded in the nanoparticles at the end of the process.

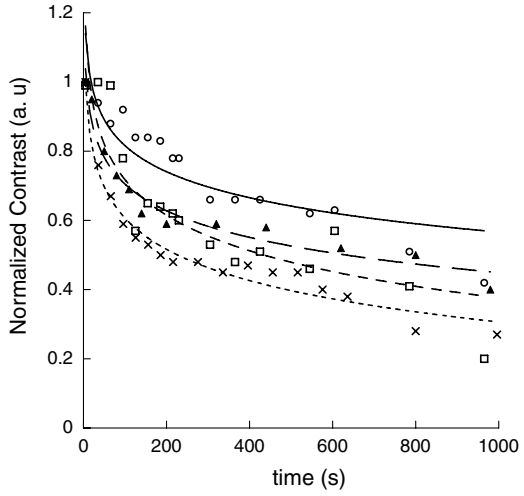

Fig. 2. The effect of mean particle size on the decay of TCPP fluorescence contrast in several nanoparticle batches of different mean NP diameter after intravenous injection of each formulation at dose of 1 mg/kg b.w. : (–○–) 121 nm, (–□–) 194 nm, (–▲–) 250 nm, (–X–) 343 nm nanoparticles.

content of around 1% was obtained with entrapment efficiencies as high as 23%.

3.2. Effect of particle size on the rate of extravasation

Fig. 2 shows the effect of the nanoparticle size on the clearance of the TCPP fluorescence from the blood vessels. The injected batches of the larger NPs are associated with more rapid clearance of the TCPP fluorescence from the vessels. One possible explanation for this observation would be that the larger nanoparticles still containing the fluorescing TCPP are taken up more rapidly than the smaller nanoparticles by the mononuclear phagocytic system (MPS). Indeed, it has been reported that the circulating time and the amount of nanocarriers such as liposomes in the blood vary depending on their uptake by cells in the reticuloendothelial system (RES), for instance macrophages [24]. Rapid elimination of the NPs from the blood stream should occur when the NPs are covered with plasma proteins. In this way they are quickly cleared by the RES before they can reach target cells. The mechanisms involved in the recognition of NP by RES have been studied by Blunk et al [25]. They have shown that poly-acrylamide gel electrophoresis (2-D PAGE) could be useful for establishing a mapping of proteins adsorbed on the surface of the NP. These and others studies point to one possible approach which would be to increase the blood circulation time of NPs by modifying the surface of the NPs by polymers like PEG. Another approach for attaining longer blood circulation times would be to decrease the size of nanocarrier in order to reduce the recognition of NPs by the RES.

Similar results to those observed in the present work were observed in a recent analysis which showed a positive correlation between the size of colloidal carriers such as liposomes and their rate of disappearance from blood vessels [26].

3.3. The effect of particle size on the photothrombic activity

It is important to make a distinction between the weight and the number of particles internalized. In general, even if big NPs are phagocytosed in lower quantity than small particles, they represent a more important total internalized mass. Rudt and Müller demonstrated, in vitro, that the mass of polystyrene particles phagocytosed by human granulocytes increased with the size of particles up to 1 μm [27]. Moreover, the degree of hepatic extraction of multilamellar liposomes seems to be linked to, and increase with their size (up to 1 μm) when the lipids administered dose is constant [28,29]. A direct investigation of the size dependence of the penetration of nanoparticles into the vessel wall reported that 514 nm NP accumulate primarily at the luminal surface of the vessel, while NP of 100 and 200 nm penetrate in the inner regions of the vessels wall [30]. As the experimental conditions of these studies, and our study, are quite different, it is difficult to establish a prediction for the photothrombic efficacy, without a direct measurement. Interestingly, blood vessels with diameters much larger than the optical penetration depth at 420 nm in blood were effectively closed, presumably due to photophysically induced biochemical processes.

The extent of vascular damage induced by the four NP batches are reported in Fig. 3. It can be observed that the photothrombic efficiency of TCPP encapsulated in NPs is particle size-dependent. Indeed, the extent of vascular closure decreased when the mean particle size increased. Fig. 4 shows that small NPs (121 nm in diameter) led to significantly higher vascular damage and closure, as compared to larger NPs (343 nm). This information might possibly be correlated to the pharmacokinetic fluorescence decay reflecting the level of TCPP circulation in blood, but the variation of the photothrombic efficacy is much higher. It might also be due to the fact that the loaded PS in the bigger particles might not be efficient to affect the endothelial cells. It may also be noted that it was previously found that the targeting of carriers to non-phagocytotic cells works for carrier sizes below 150 nm [31]. Thus, the improvement of the photothrombic efficiency of TCPP

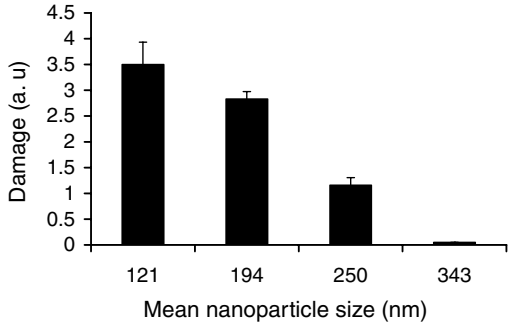

Fig. 3. The influence of the mean nanoparticle size on the photothrombic efficiency of TCPP loaded into the four nanoparticle batches. Irradiations were performed with a light fluence of 10 J/cm^2 after injection of 1 mg/kg b.w. of TCPP incorporated into each nanoparticle formulation.

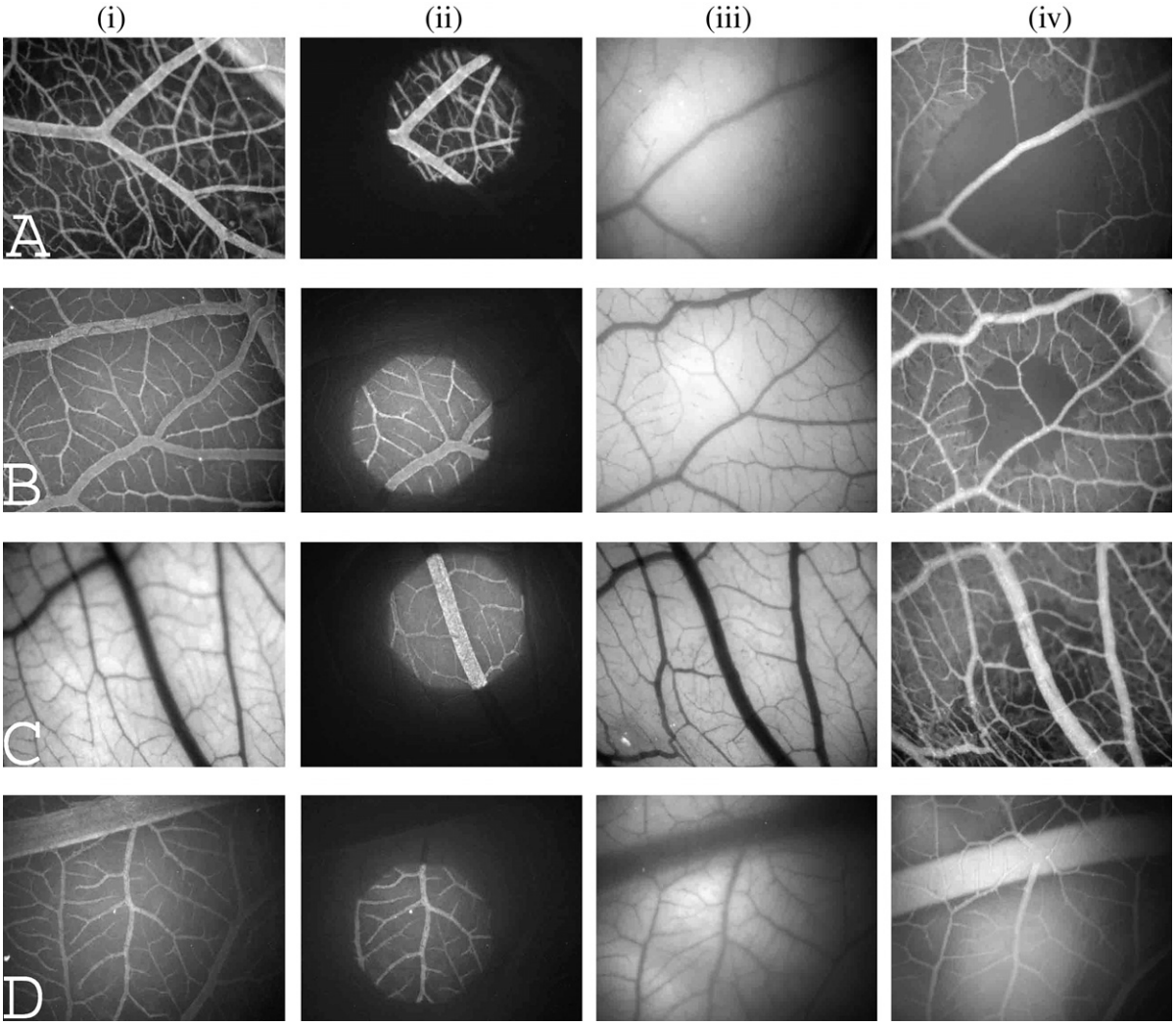

Fig. 4. Fluorescence microscopic images of PDT effects on CAM blood vessels using i.v. injection of nanoparticles at a drug dose of 1.0 mg/kg b.w. Images size are 3.51×2.81 mm. (i) 1st column for TCPP fluorescence angiography 10 s before irradiation ($\lambda_{ex} = 400$–440 nm; $\lambda_{em} > 650$ nm, exposure time 1 s) (except for C, scattered light image). (ii) 2nd column for TCPP fluorescence angiography ($\lambda_{ex} = 400$–440 nm; $\lambda_{em} > 650$ nm, exposure time 1 s) during irradiation; the diameter of the irradiated area is $\approx$1.75 mm; fluence = 10 J/cm^2. (iii) 3rd column for control scattered light image ($\lambda_{ex} = 500$–550 nm) 18 h after PDT. (iv) 4th column for sulforhodamine 101 (R101) fluorescence angiography ($\lambda_{ex} = 500$–550 nm; $\lambda_{em} > 610$ nm, exposure time 1 s) showing the vascular occlusion induced in the circular irradiated area 18 h after PDT. (A: $\varnothing = 121$ nm, B: $\varnothing = 194$ nm, C: $\varnothing = 250$ nm, D: $\varnothing = 343$ nm) illustrating the vessel closure also indicated in Fig. 3.

mediated by its encapsulation into the smaller sized NPs (121 in diameter) might be due to more effective drug delivery to the endothelial cells. NPs with the smaller mean size (i.e. 121 nm) are thus preferable.

4. Conclusion

From the data reported above, several trends are apparent. First, the mean size of the NPs under the applied conditions appears to be a parameter that governs the duration of the circulation of the NP-delivered photosensitizer in bloodstream. The size of the nanoparticle carrier may influence the photothrombic efficiency both by keeping the TCPP longer in the bloodstream where it does the photodynamic damage and may help the targeting of the TCPP to the right spot on/in the endothelium. Thus nanoparticle size may be a key in determining the photothrombic efficiency of entrapped TCPP and in designing more effective NP-delivered photosensitizers. Overall, smaller nanoparticle size, under the applied conditions, clearly increases the activity of the encapsulated photosensitizing agent.

5. Abbreviations

AMD	age-related macular degeneration
b.w.	body weight
CAM	chorioallantoic membrane
CNV	choroidal neovascularization
DMSO	dimethylsulfoxide

EDD	day of embryo development
i.v.	intravenously
MPS	mononuclear phagocytic system
NPs	nanoparticles
PBS	phosphate buffer saline
PDT	photodynamic therapy
PSs	photosensitizers
PVAL	poly(vinyl alcohol)
RES	reticuloendothelial system
TCPP	*meso-tetra*(carboxyphenyl)porphyrin

References

[1] N.M. Bressler, Verteporfin therapy of subfoveal choroidal neovascularization in age-related macular degeneration: two-year results of a randomized clinical trial including lesions with occult with no classic choroidal neovascularization–verteporfin in photodynamic therapy report 2, Am. J. Ophthalmol. 133 (2002) 168–169.

[2] N.M. Bressler, S.B. Bressler, S.L. Fine, Age-related macular degeneration, Surv. Ophthalmol. 32 (1988) 375–413.

[3] R.Z. Renno, J.W. Miller, Photosensitizer delivery for photodynamic therapy of choroidal neovascularization, Adv. Drug Deliv. Rev. 52 (2001) 63–78.

[4] E. Allemann, J. Rousseau, N. Brasseur, S.V. Kudrevich, K. Lewis, J.E. van Lier, Photodynamic therapy of tumours with hexadecafluoro zinc phthalocynine formulated in PEG-coated poly(lactic acid) nanoparticles, Int. J. Cancer 66 (1996) 821–824.

[5] Y.N. Konan, M. Berton, R. Gurny, E. Allemann, Enhanced photodynamic activity of *meso-tetra*(4-hydroxyphenyl)porphyrin by incorporation into sub-200 nm nanoparticles, Eur. J. Pharm. Sci. 18 (2003) 241–249.

[6] B. Pegaz, E. Debefve, F. Borle, J.P. Ballini, H. van den Bergh, Y.N. Kouakou-Konan, Encapsulation of porphyrins and chlorins in biodegradable nanoparticles: the effect of dye lipophilicity on the extravasation and the photothrombic activity. A comparative study, J. Photochem. Photobiol. B 80 (2005) 19–27.

[7] A. Vargas, B. Pegaz, E. Debefve, Y. Konan-Kouakou, N. Lange, J.P. Ballini, H. van den Bergh, R. Gurny, F. Delie, Improved photodynamic activity of porphyrin loaded into nanoparticles: an in vivo evaluation using chick embryos, Int. J. Pharm. 286 (2004) 131–145.

[8] Y. Konan-Kouakou, R. Boch, R. Gurny, E. Allemann, In vitro and in vivo activities of verteporfin-loaded nanoparticles, J. Controlled Release 103 (2005) 83–91.

[9] M.J. Hammer-Wilson, L. Akian, J. Espinoza, S. Kimel, M.W. Berns, Photodynamic parameters in the chick chorioallantoic membrane (CAM) bioassay for topically applied photosensitizers, J. Photochem. Photobiol. B 53 (1999) 44–52.

[10] D. Ribatti, B. Nico, A. Vacca, L. Roncali, P.H. Burri, V. Djonov, Chorioallantoic membrane capillary bed: a useful target for studying angiogenesis and anti-angiogenesis in vivo, Anat. Rec. 264 (2001) 317–324.

[11] H. Toledano, R. Edrei, S. Kimel, Photodynamic damage by liposome-bound porphycenes: comparison between in vitro and in vivo models, J. Photochem. Photobiol. B 42 (1998) 20–27.

[12] N. Lange, J.P. Ballini, G. Wagnieres, H. van den Bergh, A new drug-screening procedure for photosensitizing agents used in photodynamic therapy for CNV, Invest. Ophthalmol. Vis. Sci. 42 (2001) 38–46.

[13] B. Pegaz, E. Debefve, F. Borle, J.P. Ballini, G. Wagnieres, S. Spaniol, V. Albrecht, D. Scheglmann, N.E. Nifantiev, H. van den Bergh, Y.N. Konan, Preclinical evaluation of a novel water-soluble chlorin E6 derivative (BLC 1010) as photosensitizer for the closure of the neovessels, Photochem. Photobiol. 81 (2005) 1505–1510.

[14] E. Allemann, E. Doelker, R. Gurny, Drug loaded poly (Lactic Acid) nanoparticles produced by a reversible salting-out process - purification of an injectable dosage form, Eur. J. Pharm. Biopharm. 39 (1993) 13–18.

[15] E. Allemann, R. Gurny, E. Doelker, Preparation of aqueous polymeric nanodispersions by a reversible salting-out process - influence of process parameters on particle-size, Int. J. Pharm. 87 (1992) 247–253.

[16] H. Ibrahim, C. Bindschaedler, E. Doelker, P. Buri, R. Gurny, Aqueous nanodispersions prepared by a salting-out process, Int. J. Pharm. 87 (1992) 239–246.

[17] D. Quintanar-Guerrero, E. Allemann, H. Fessi, E. Doelker, Preparation techniques and mechanisms of formation of biodegradable nanoparticles from preformed polymers, Drug Dev. Ind. Pharm. 24 (1998) 1113–1128.

[18] F. De Jaeghere, E. Allemann, J.C. Leroux, W. Stevels, J. Feijen, E. Doelker, R. Gurny, Formulation and lyoprotection of poly (lactic acid-co-ethylene oxide) nanoparticles: influence on physical stability and in vitro cell uptake, Pharm. Res. 16 (1999) 859–866.

[19] J.F. Carpenter, M.J. Pikal, B.S. Chang, T.W. Randolph, Rational design of stable lyophilized protein formulations: some practical advice, Pharm. Res. 14 (1997) 969–975.

[20] Y.N. Konan, R. Gurny, E. Allemann, Preparation and characterization of sterile and freeze-dried sub-200 nm nanoparticles, Int. J. Pharm. 233 (2002) 239–252.

[21] J.C. Leroux, F. De Jaeghere, B. Anner, E. Doelker, R. Gurny, An investigation on the role of plasma and serum opsonins on the internalization of biodegradable poly (D,L-lactic acid) nanoparticles by human monocytes, Life Sci. 57 (1995) 695–703.

[22] A.L. Romanoff, Biochemistry of the Avian Embryo: A Quantitative Analysis of Prenatal Development, John Wiley & Sons, New York, 1967.

[23] J.C. Leroux, E. Allemann, E. Doelker, R. Gurny, New approach for the preparation of nanoparticles by an emulsification–diffusion method, Eur. J. Pharm. Biopharm. 41 (1995) 14–18.

[24] A.N. Kazuko Uchiyama, Yumiko Yamagiwa, Tomoyo Nishida, Hideyoshi Harashima, Hiroshi Kiwada, Effects of the size and fluidity of liposomes on their accumulation in tumors: a presumption of their interaction with tumors, Int. J. Pharm. 121 (1995) 195–203.

[25] T. Blunk, D.F. Hochstrasser, J.C. Sanchez, B.W. Muller, R.H. Muller, Colloidal carriers for intravenous drug targeting: plasma protein adsorption patterns on surface-modified latex particles evaluated by two-dimensional polyacrylamide gel electrophoresis, Electrophoresis 14 (1993) 1382–1387.

[26] H. Harashima, H. Kiwada, Liposomal targeting and drug delivery: kinetic consideration, Adv. Drug Deliv. Rev. 19 (1996) 425–444.

[27] S. Rudt, R.H. Muller, Invitro phagocytosis assay of nanoparticles and microparticles by chemiluminescence .1. effect of analytical parameters, particle-size and particle concentration, J. Controlled Release 22 (1992) 263–271.

[28] H. Harashima, Y. Ohnishi, H. Kiwada, In vivo evaluation of the effect of the size and opsonization on the hepatic extraction of liposomes in rats: an application of Oldendorf method, Biopharm. Drug Dispos. 13 (1992) 549–553.

[29] H. Harashima, K. Sakata, H. Kiwada, Distinction between the depletion of opsonins and the saturation of uptake in the dose-dependent hepatic uptake of liposomes, Pharm. Res. 10 (1993) 606–610.

[30] U. Westedt, L. Barbu-Tudoran, A.K. Schaper, M. Kalinowski, H. Alfke, T. Kissel, Deposition of nanoparticles in the arterial vessel by porous balloon catheters: localization by confocal laser scanning microscopy and transmission electron microscopy, AAPS. Pharm. Sci. 4 (2002) E41.

[31] R. Maassen, Mesoscopic particles in polymer solutions, thesis 2002, uni-duesseldorf (DE).